K.T. McDonald
Princeton U.
Dec. 3, 1992

Silicon Calorimetry in E-144

In this note we review the role of silicon calorimetry in E-144 and sketch our present understanding of the desired configuration of the calorimeters.

There are three possible applications of calorimetry to E-144:

1. As the energy/position-sensitive device to detect positrons produced at the e-laser interaction point.

2. As the energy/position-sensitive device to observe electrons scattered at the e-laser interaction point.

3. As a total-energy/quadrant monitor for high-energy photons backscattered from the e-laser interaction point.

The configuration of calorimeters for applications 1 and 2 depends on the layout of the dump magnets, which is discussed in the following section. Then we propose configurations of the calorimeters in sec. 2.

We anticipate that the silicon calorimeters will be based on wafers designed at U. Tennessee that are 6.4×6.4 cm^2 each, with 16 square pads per wafer. Calorimeter modules would consist of 20 radiation length of tungsten with one silicon wafer per radiation length. The readout of each pad 'tower' would be grouped into two longitudinal segments, perhaps 10 radiation lengths each. We will find below that it is sufficient to read out only the central two columns of pads in our application, as all particles of interest in E-144 as dispersed over a vertical strip only 2-3 mm wide.

The tentative calorimeter configuration is then:

1. A positron calorimeter consisting of four modules, with 32 towers and 64 channels read out.

2. An electron calorimeter consisting of three modules, with 24 tower and 48 channels read out.

3. A photon beam calorimeter consisting of a single modules with perhaps only 4 towers and 8 channels read out.

In total there would be eight calorimeter modules, requiring 160 wafers, with 120 channels of electronics.

1 $e^{\pm}$ Trajectories in the Dump-Magnet String

Immediately following the e-laser interaction point the 50-GeV electron beam is pitched ≈ 19 mrad downwards into a dump by a string of eight magnets. This dump-magnet string is reasonably well-defined at present as consisting of

1. A 1.2-m-long trim electromagnet with a 50-μrad kick.
2. A 1.2-m-long trim electromagnet with a 500-μrad kick.
3. Six 1-m-long permanent C-magnets with a 3-mrad kick each. The 'C' opens upwards. End and side views of these magnets or shown in Figs. 1 and 2. These magnets are being remapped; an old map of the variation of the field with height (in the midplane) is shown in Fig. 3. There was considerable variation in the field shape from magnet to magnet, and an asymmetry in the shape that is not understood by me.

Fig. 4 shows a near-final layout of these eight magnets, and trajectories through them of electron and positrons of various energies. The trajectories were calculated by A. Melissinos and colleagues, and I do not have precise details on the field shape in the C-magnet they used, but it is based on Fig. 3.

2 Positron Calorimeter

In E-144 we should be able to detect positrons from the two-stage process

$$e + \omega_0 \to e' + \omega, \qquad \text{followed by} \qquad \omega + n\omega_0 \to e^+e^-, \tag{1}$$

in which a laser photon of frequency ω_0 is backscattered to energy ω, and this high-energy photon collides with n laser photons before leaving the interaction region. For this process to be probable, the electric field strength of the laser must approach the QED critical field

$$E_{\rm crit} = \frac{m^2c^3}{e\hbar} = 1.32 \times 10^{16}\ \text{V/cm} = 4.41 \times 10^{13}\ \text{gauss} \tag{2}$$

in the rest frame of the beam electron. Such fields will also be encountered at the surface of a beam bunch at a future e^+e^- linear collider, where the ensuing radiation is termed beamstrahlung. Hence positron production in E-144 can be considered as a preview of beamstrahlung e^+e^- creation, which provides one motivation for our measurement.

We first discuss the range of positron energies and angles that will occur in E-144 as a guide for design of the positron spectrometer.

2.1 Positron Energy

In sec. 6 of the E-144 proposal we remarked on the care that must be taken when considering the kinematics of pair production in a strong laser field because of the difference between the 4-vectors of the particles inside and out of the strong-field region. However, the main subtlety is in the pair mass, and not so much in the kinematics of the electron and

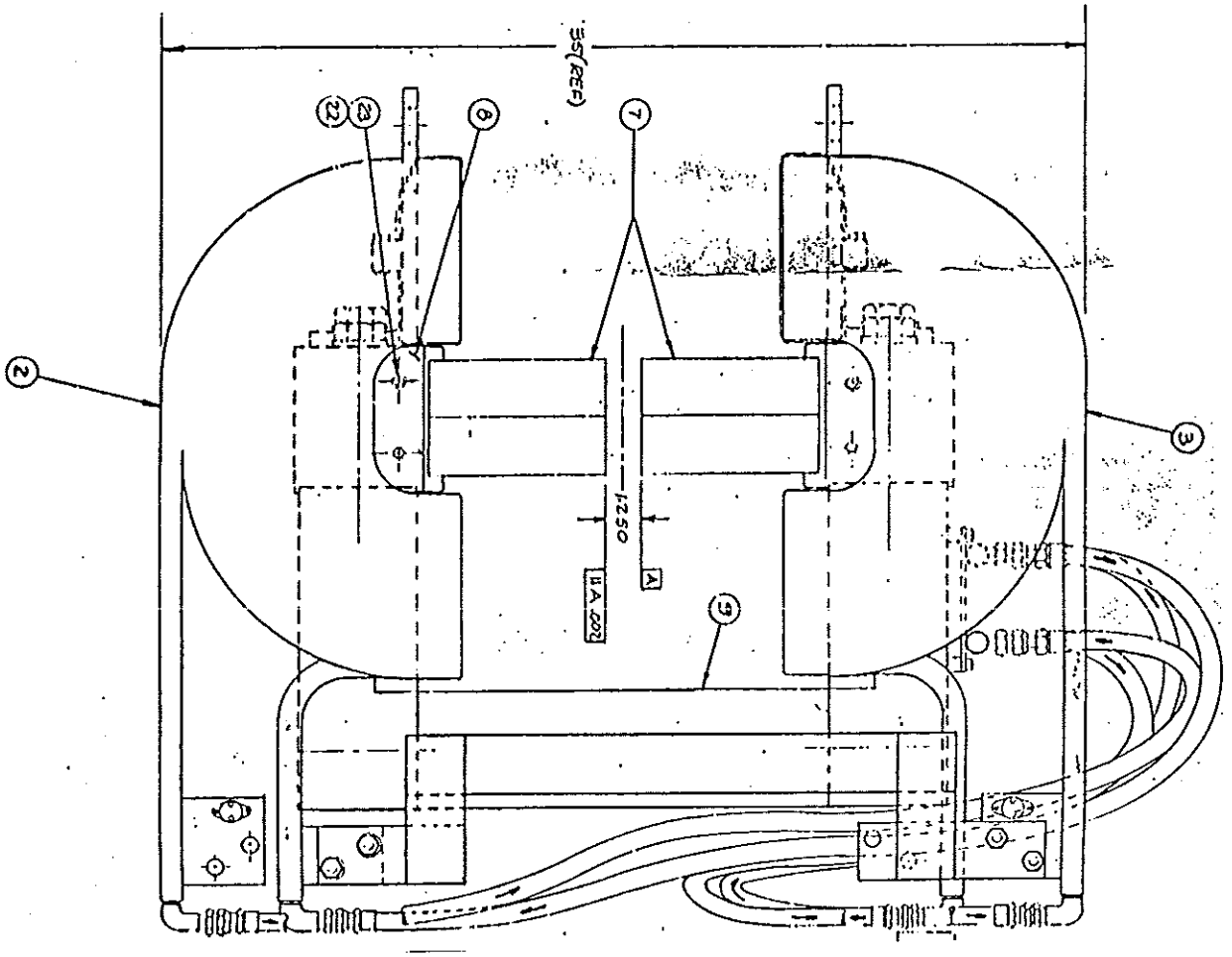

Figure 1: End view of the permanent C-magnets. The gap is 1.25″ wide, the pole tips are 4″ high, and the distance from the bottom of the pole tips to the top of the yoke is 8″. The coils labelled 3 are used only to excite the permanent magnets initially, and are off during normal use. The horizontal gap between the coils is 12″.

positron separately. In this note we are primarily concerned with the positron only, as the beamstrahlung experiment will not detect coincidences between the electron and positron.

Recall that if p is the 4-vector of a positron (or electron) in the field-free region, its 4-vector $\overline{p}$ inside a plane-wave field of strength $\eta \equiv eE/m\omega_0 c$ can be written

$$\overline{p} = p + \kappa\omega_0, \qquad \text{where} \qquad \kappa = \frac{m^2\eta^2}{2(p\cdot\omega_0)}, \tag{3}$$

and the positron mass inside the field is $\overline{m} = m\sqrt{1+\eta^2}$. This assumes the particles leave the field across a region where the gradient of field intensity is parallel to the particles' momenta. In the following subsection we verify that this is a good approximation. For example, if $p_0 = 5$ GeV, and p is opposite to k_0 then $\kappa = 1.2\eta^2$ for a laser with $\lambda = 1.06$ μm.

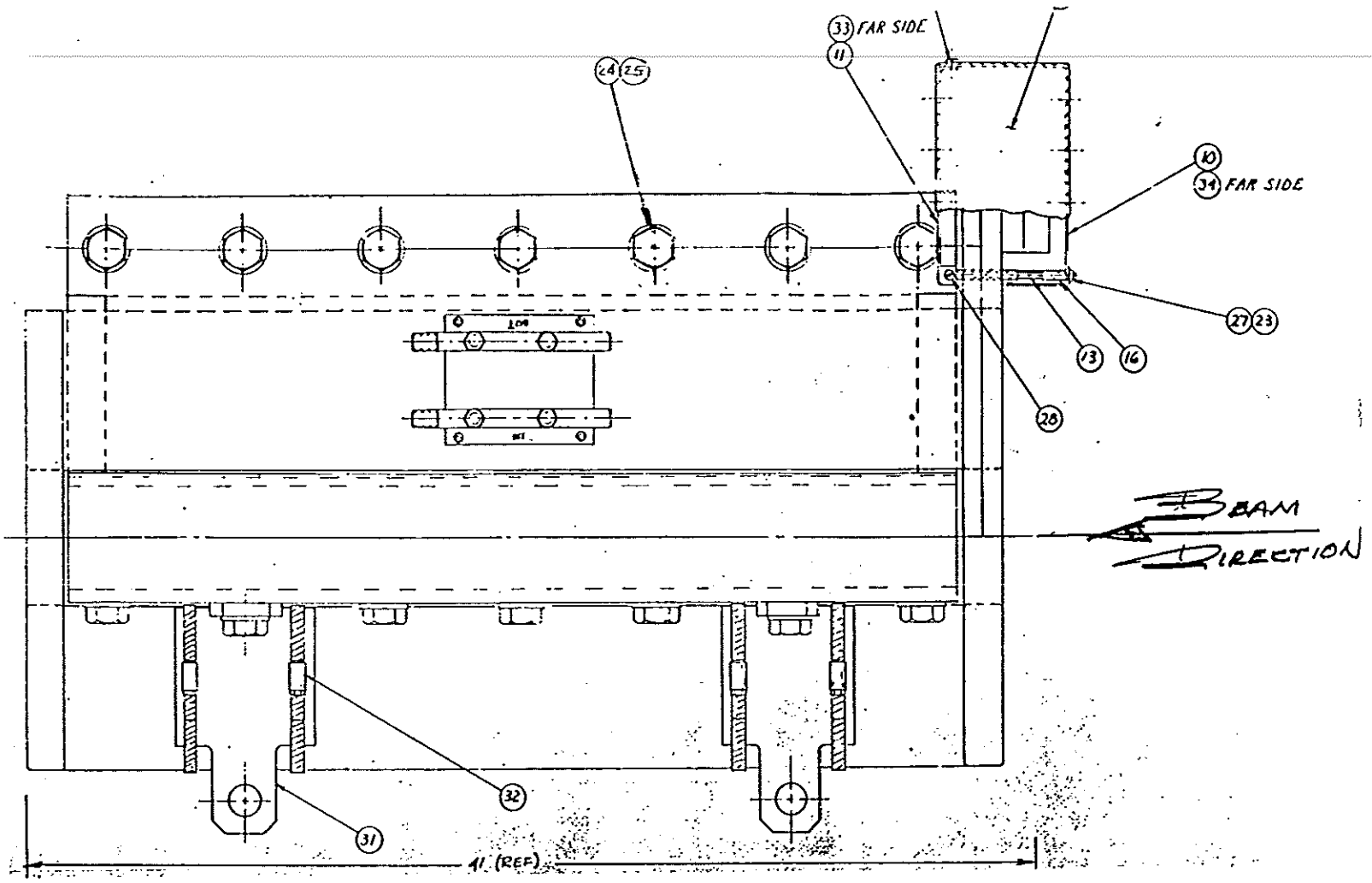

Figure 2: Side view of the permanent C-magnets. The pole tips are 36″ long, while the coils extend over 41″.

In E-144 the laser may achieve $\eta \approx 2.5$, so $\kappa \lesssim 8$ for positrons of interest. In this case the distinction between $\overline{p}$ and p is unmeasurably small (so long as we only study the positron).

The pair $\overline{p}_1 + \overline{p}_2$ is created in the collision of a high energy photon ω with n laser photons ω_0 so the pair invariant mass can be written

$$\overline{M}^2 \equiv (\overline{p}_1 + \overline{p}_2)^2 = 4n\omega\omega_0, \tag{4}$$

assuming a head-on collision. The threshold condition is that the center-of-mass energy be $2\overline{m} = 2m\sqrt{1+\eta^2}$ and not $2m$ as for a field-free region. In E-144 we are never far from threshold, so $\overline{M}$ is always in the range 1-10 MeV/c^2.

In the center-of-mass frame (= pair rest frame, labelled by a $\star$) the positron is created with energy and momentum given by

$$\overline{p}_0^\star = \overline{M}/2, \qquad \overline{p}^\star = \sqrt{\overline{p}_0^{\star} - \overline{m}^2}. \tag{5}$$

Noting the smallness of κ in eq. (3), in the remainder of this subsection and in the following subsection we write the positron momentum as p, although strictly speaking our derivations

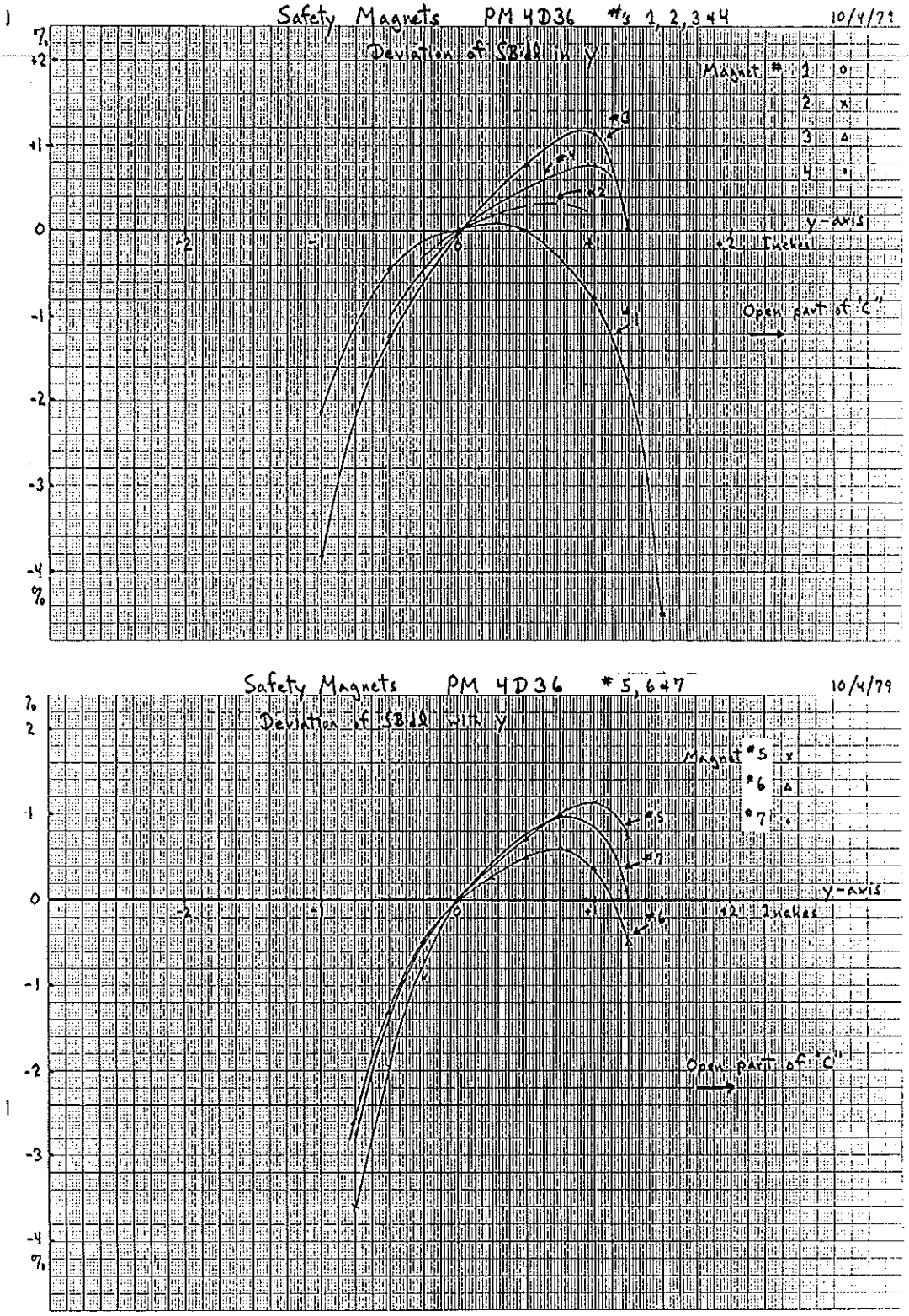

Figure 3: Maps of the variation with height of the field strength in the midplane of the permanents magnets (only 6 of which are available for E-144).

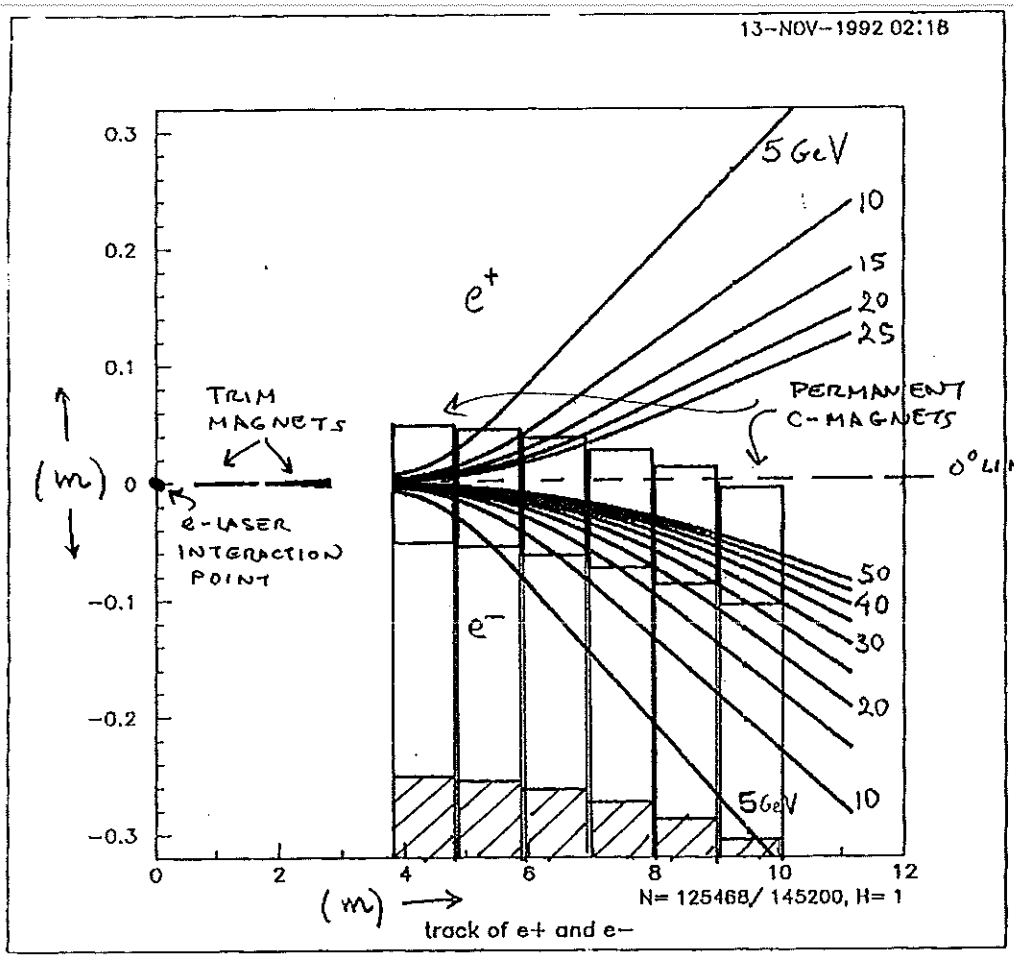

Figure 4: Side view of the layout of the eight dump magnets, with various electron and positron trajectories as calculated by A. Melissinos *et al.*

are for $\overline{p}$. Thus we rewrite eq. (5) as

$$p_0^\star = \overline{M}/2, \qquad p^\star = \sqrt{p_0^{\star} - \overline{m}^2}. \tag{6}$$

However, we cannot replace $\overline{m}$ by m in eq. (6)! The velocity of the positron in the pair rest frame is

$$\beta^\star = \frac{p^\star}{p_0^\star} = \sqrt{1 - \frac{4\overline{m}^2}{\overline{M}^2}} = \sqrt{1 - \frac{m^2(1+\eta^2)}{n\omega_0\omega}}, \tag{7}$$

which is significantly less than 1 in E-144.

The transformation from the pair rest frame to the lab has

$$\gamma = \frac{\omega + n\omega_0}{\overline{M}} \approx \frac{\omega}{\overline{M}}, \qquad \beta \approx 1. \tag{8}$$

Thus the maximum and minimum energies of the positron in the lab frame are then

$$p_{0,\mathrm{max,min}} = \gamma(p_0^* \pm \beta p^*) \approx \frac{\omega}{2}\left(1 \pm \sqrt{1 - \frac{m^2(1+\eta^2)}{n\omega_0\omega}}\right). \tag{9}$$

The energy spectrum is symmetric about half the energy of the high-energy photon, and does not extend down to zero because the positron is nonrelativistic in the pair rest frame. Just above threshold the spectrum is confined to the vicinity of $\omega/2$. The smallest values of $p_{0,\mathrm{min}}$ come when the production is well above threshold, and we approximate eq. (9) as

$$p_{0,\mathrm{min}} \approx \frac{m^2(1+\eta^2)}{4n\omega_0}, \tag{10}$$

independent of ω of the high-energy photon. However, there is a spectrum of laser photon numbers n contributing to pair creation, so the minimum positron energy depends on the dynamics of pair creation, not just kinematics. From numerical calculations presented below we find that for η slightly greater than one typical values of n are $4\eta^3$. Hence $p_{0,\mathrm{min}} \approx m^2/16\eta\omega_0 \approx 15\ \mathrm{GeV}/\eta$ for $\omega_0 = 1.17$ eV. With $\eta \approx 3$ in E-144, we expect the minimum positron energy to be about 5 GeV.

We illustrate the above estimates with numerical calculations of the positron-production cross section by circularly polarized photons using expressions for the cross section given by Narozhnyi *et al.* [1]. The Fortran code is in a file called SIGTHOMBW.FOR. Figure 5 shows calculations for high-energy photons of various energies between 11 and 30 GeV colliding with laser photons of wavelength 1.06 μm. The assumed laser intensity corresponds to a 4-Joule pulse of 1 psec FHWM focused with an $f/D = 5$ mirror, as should be available in the first phase of E-144. Figure 6 shows a similar calculation for frequency-doubled laser photons, assuming a rather optimistic pulse energy of 16 Joules (or 8 Joules in a pulse shortened to 0.5 psec FWHM).

We infer that there will be little positron production for energies below 3-4 GeV, in agreement with the preceding estimates.

The maximum positron energy can also be inferred from the figures on noting that the endpoint energy for ordinary Compton scattering of 50-GeV electrons and 1.06-μm photons is 23 GeV, or 32 GeV with 0.53-μm photons. In practice there will be little pair creation from backscattered photons beyond the ordinary Compton endpoint due on nonlinear Compton scattering. Hence for 1.06-μm laser photons the maximum positron energy is around 17 GeV, while with 0.53-μm photons it is about 24 GeV.

For very intense laser beams the positrons may suffer Compton scattering as they leave the interaction region, which would degrade their energy below the preceding values. Hence there may be some interest in detecting positrons at energies lower than the nominal kinematic limit of 3 or so GeV.

2.2 Positron Angle

The transverse dimensions of the positron spectrometer should be set by the maximum angle θ_{max} between the positron and the high-energy photon.

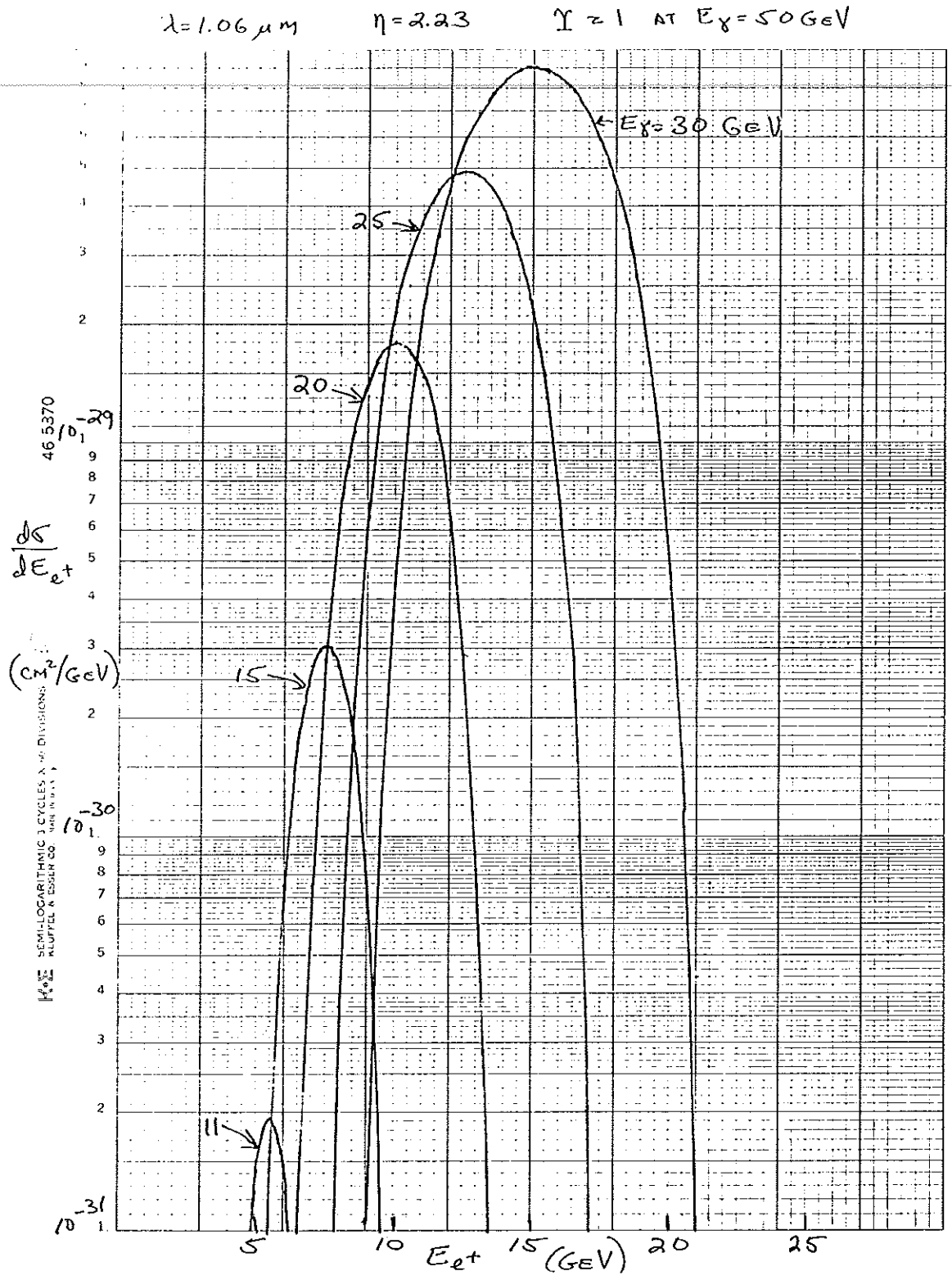

Figure 5: Calculations of the positron-production cross section $d\sigma/dE_{e^+}$ for photons of energies from 11 to 30 GeV colliding with circularly polarized laser photons of 1.06-μm wavelength. The laser is considered as a plane wave with intensity parameter $\eta = 2.23$.

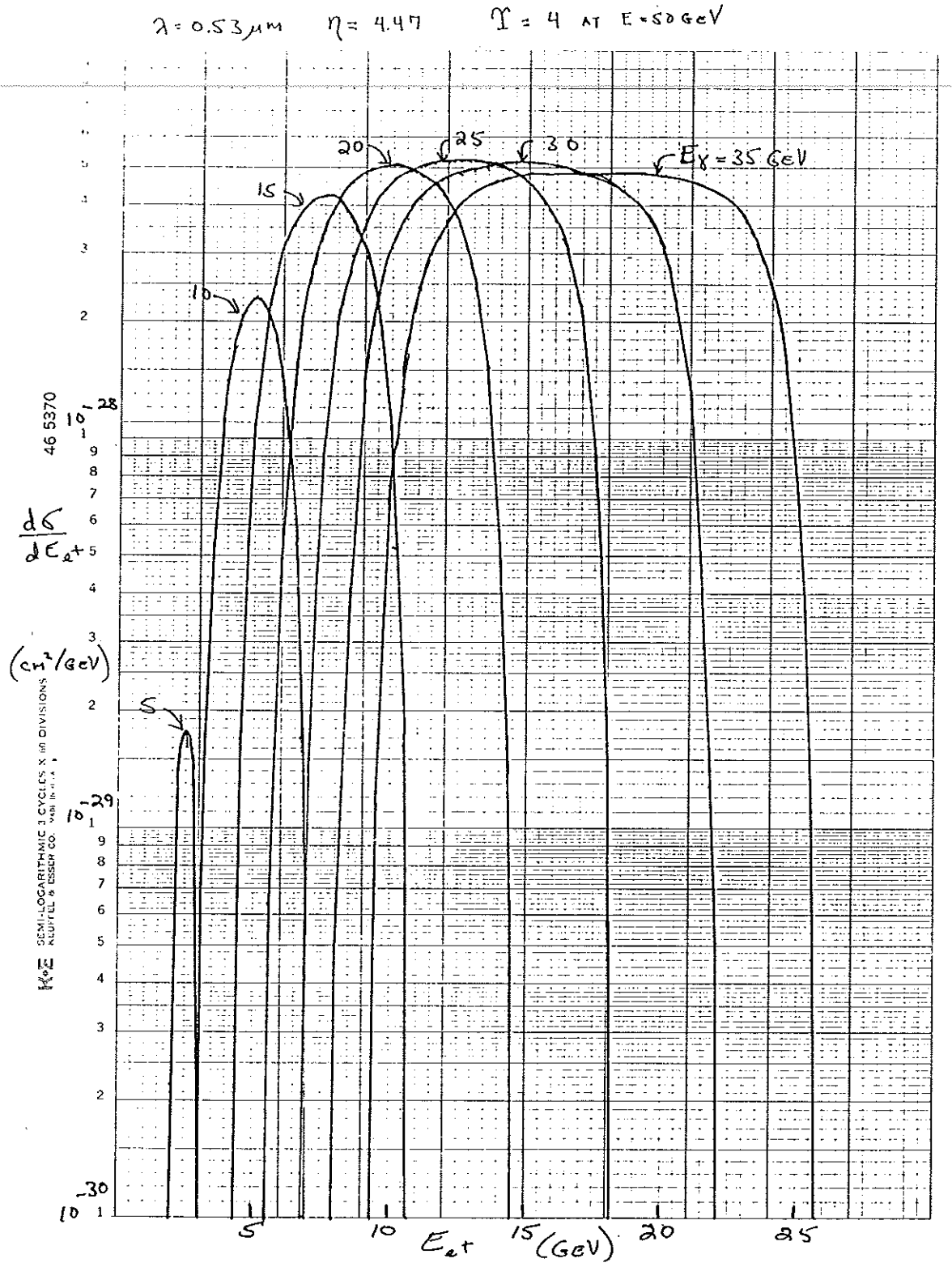

Figure 6: Calculations of the positron-production cross section $d\sigma/dE_{e^+}$ for photons of energies from 5 to 35 GeV colliding with circularly polarized laser photons of 0.53-μm wavelength. The laser is considered as a plane wave with intensity parameter $\eta = 4.47$.

Using the notation of the previous subsection,

$$\tan\theta = \frac{p_\perp}{p_\parallel} \approx \frac{p^\star \sin\theta^\star}{\gamma(p_0^\star + p^\star\cos\theta^\star)}, \tag{11}$$

where $\theta^\star$ is the angle between the positron in the pair rest frame and the high-energy photon in the lab. Both $\theta^\star = 0$ and π lead to $\theta = 0$, so there is a maximum lab angle $\theta_{\rm max}$, sometimes called the Jacobean peak, which is of order $1/\gamma$.

Setting the derivative of $\tan\theta$ with respect to $\cos\theta^\star$ to zero we find

$$\cos\theta^\star_{\rm max} = -\beta^\star, \quad \sin\theta^\star_{\rm max} = \frac{\overline{m}}{p_0^\star}, \quad \tan\theta_{\rm max} = \frac{p_0^\star\beta^\star}{\gamma\overline{m}} = \frac{2n\omega_0}{m\sqrt{1+\eta^2}}\beta^\star \le \frac{2n\omega_0}{m\sqrt{1+\eta^2}}. \tag{12}$$

As with eq. (10) for $p_{0,\rm min}$, our expression for $\theta_{\rm max}$ does not depend explicitly on the energy ω of the high-energy photon, although the dependence on the dynamical variable n contains ω implicitly. Using $n \approx 4\eta^3$ as a typical value when η is slightly greater than 1, we estimate that

$$\theta_{\rm max} \approx \frac{8\eta^2\omega_0}{m} \approx 165\ \mu{\rm rad}, \qquad (\eta = 3,\ \omega_0 = 1.17\ {\rm eV}). \tag{13}$$

If the positron spectrometer is located, say, 8 m downstream of the collision point, then the positrons extend only about ± 1.3 mm transversely. Note, however, that the maximum extent is a rapid function of η, so increased laser power will require considerably large transverse coverage.

2.3 Configuration of the Positron Spectrometer

Figure 7 shows a layout of the dump-magnet string including placement of a silicon calorimeter for positron detection just after the fourth permanent magnet. At this location 25-GeV positrons are 5 cm above the 0° beamline, which we judge is sufficient clearance for the vacuum pipe that must extend downstream.

We propose to use a silicon calorimeter based on the U. Tennessee silicon wafers whose size is 6.4×6.4 cm^2. Four modules stacked vertically would permit detection of positrons down to about 3 Gev, three modules would cut off the spectrum at about 4 GeV, while five modules would extend to coverage to nearly 2 GeV.

To keep the positrons from showering in the vacuum chamber its wall must be vertical just upstream of the calorimeter. This leads to mechanical constraints as to the extent of the chamber, which are still being evaluated by D. Walz. It would be very desirable to have at least four calorimeter modules in the positron spectrometer, which requires the vacuum chamber to extend about 32 cm above the beamline.

The transverse spread of the positrons over the face of the calorimeter is small enough that the option exists to only instrument the central 50% of each module, as mentioned in previous notes.

When the experiment first works well enough that positrons can be observed the rate will be only one or less per pulse. However, when the experiment performs at design luminosity we must expect 1000 or more positrons in the calorimeter each pulse. This will likely require a second set of preamplifiers for the calorimeter with suitably reduced gain. The other two calorimeters described below will in general have even higher rates than the positron calorimeter.

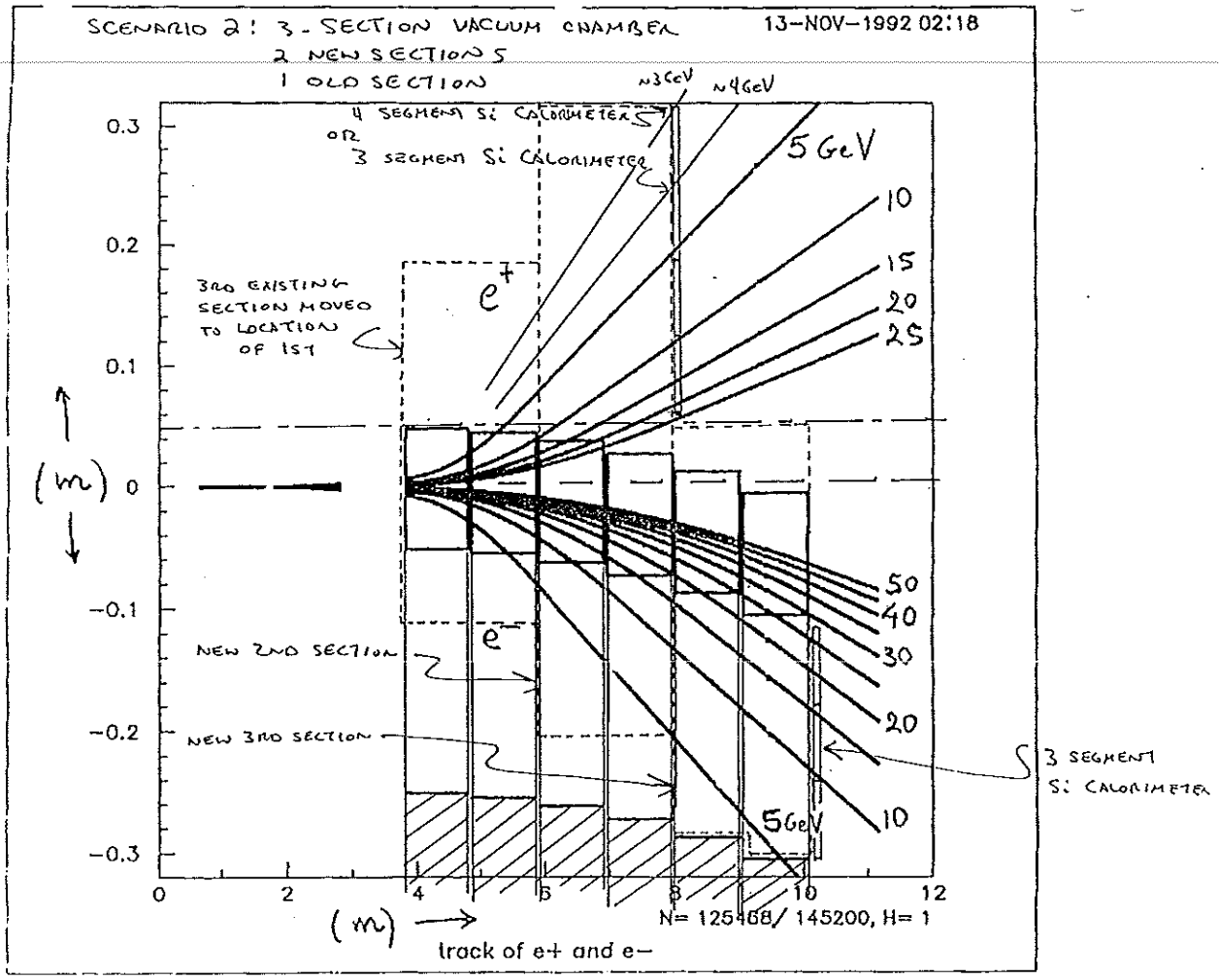

Figure 7: Side view of the layout of the eight dump magnets, showing the proposed location of a 4-module silicon calorimeter for positrons, and a three-module calorimeter for scattered electrons.

3 Electron Calorimeter

The configuration of the dump-magnet string is favorable for measurement of scattered electrons of energies between 6 and 30 GeV, supposing the upper limit is set by a requirement that any detector remain 5 cm below the primary beam (see Fig. 7). A silicon calorimeter consisting of three modules of U. Tennessee wafers would fit well just downstream of the sixth dump magnet in the short free space upstream of the γ-laser interaction point.

The physics interest in such a calorimeter is twofold.

3.1 Nonlinear Compton Scattering

As noted in sec. 1.1 above, the maximum photon energy from ordinary Compton scattering of a 50-GeV electron with 1.06-μm photons is 23 GeV, so the corresponding minimum energy

for the scattered electron is 27 GeV. For 0.53-μm laser photons the minimum electron energy is 18 GeV.

Electrons of energies lower that this 'minimum' can occur either due to multiple ordinary Compton scattering, or nonlinear Compton scattering in which several laser photons interact with an electron simultaneously. While rates for the two processes are similar, it will be interesting to see if we can detect a signal for nonlinear Compton scattering by measurement of the electron rather than the photon. (The photon spectrometer will likely not be available during the initially running of E-144 in the latter half of 1993.) For this it is, of course, essential to have electron detection at lower energies.

3.2 Compton Polarimetry

The electron beam in the FFTB is anticipated to have sizable longitudinal polarization, measurement of which is useful for the accelerator-physics program. The polarization of the SLC beams is now determined by Compton polarimeters located in the SLC arcs, which will not be operable during FFTB running. Hence it is desirable to include a Compton polarimeter in the E-144 configuration.

The silicon calorimeter just proposed for electron detection is excellent for this purpose. The important energy range for polarimetry is just abbove the ordinary Compton endpoint. With 1.06-μm laser photons this is at 27 GeV, which energy is barely deflected by 5 cm at the end of the dump-magnet string. Some thought will be required as to whether it is wise to place the detector closer to the beam to gain better acceptance for the polarimetry measurement.

It appears that the E-144 configuration will probably not permit detection of the zero in the polarization asymmetry that occurs for photons scattered by 90° in the rest frame of the initial electron [2]. That is, the asymmetry vanishes for scattered electron energy

$$E = \frac{E_0}{1 + 2E_0\omega_0/m^2}. \tag{14}$$

For electron energy $E_0 = 50$ GeV and 1.06-μm laser photons (whose energy is 1.17 eV) the asymmetry vanishes for $E = 0.7E_0 = 35$ GeV, for which the trajectories remain very close to the unscattered beam. For frequency-doubled laser photons the asymmetry vanishes for $E = 0.54E_0 = 27$ GeV, so the zero may be observable in this case.

I believe that no calculation has been made for nonlinear Compton scattering with polarized electrons. The polarization asymmetry for electrons of energy lower than the ordinary Compton endpoint might be an interesting way to distinguish nonlinear Compton scattering from double Compton scattering.

4 0° Photon Calorimeter

It will also be desirable to have a monitor of the total energy of backscattered photons, located at the downstream end of the experiment. This function could be accomplished by a single module of the U. Tennessee silicon calorimeter. As the calorimeter is segmented

into quadrants, estimates of the horizontal and vertical centroid of the photon beam will be readily available as a diagnostic for beam steering.

It is also proposed that a CCD be used in conjunction with the calorimeter to provide a finer-resolution diagnostic of the photon beam position.

Recall that the characteristic angular width of the backscattered photon beam is $m/E_0 \approx 10^{-5}$, so that the half width of the beam at 100 m from the interaction point is 1 mm. If we desire a steering accuracy of 1 μrad (which may be excessive), then we need 0.1-mm position resolution in the photon-beam diagnostic. This is finer than can be obtained from a single shower in the silicon calorimeter, so the CCD detector could be important at low intensities. For intensities of more than 100 backscattered photons per pulse the calorimeter alone may provide all desired position resolution for steering.

5 Appendix: Υ and Electron-Photon Processes in Strong Fields

Discussion of beamstrahlung in sec. 4 of the E-144 proposal, and also in the paper of Chen and Telnov [3] on which sec. 4 is based, was perhaps insufficiently clear on the relation between strong-field processes in a laser and in static fields. This subject has been treated in some detail by Nikishov and Ritus, particularly in refs. [4] and [5] and summarized in the final paragraph of sec. 101 of ref. [6]. Sokolov and Ternov have also discussed this [7, 8], but with less clarity about the role of the invariant called Υ below.

5.1 Emission of a Photon by an Electron

It is claimed that the emission of a photon by an unpolarized electron in any constant (in both space and time) electromagnetic field can be expressed in terms of a universal expression (for example eq. (90.23) of ref. [6]) so long as the fields in the laboratory are small compared to to the QED critical field strength

$$E_{\rm crit} = \frac{m^2c^3}{e\hbar} = 1.32 \times 10^{16}\ {\rm V/cm} = 4.41 \times 10^{13}\ {\rm gauss}. \tag{15}$$

In the universal expression the dependence of the radiation on the electron momentum and electromagnetic field strength is via magnitude of the electric field in the rest frame of the electron (since in this frame where the electron has no velocity there is no magnetic effect). This is usefully written in the invariant form

$$\Upsilon = \frac{E^*}{E_{\rm crit}} = \frac{\sqrt{(p_0\mathbf{E} + \mathbf{p}\times\mathbf{B})^2 - (\mathbf{p}\cdot\mathbf{E})^2}}{mE_{\rm crit}} = \frac{|p_\mu F^{\mu\nu}|}{mE_{\rm crit}}, \tag{16}$$

where $p_\mu = (p_0, \mathbf{p})$ is the 4-vector of the electron, and we set $\hbar = c = 1$.

In a constant magnetic field

$$\Upsilon = \gamma B/E_{\rm crit} \qquad \text{(constant magnetic field)}, \tag{17}$$

where $\gamma = p_0/m$, but in a constant crossed field where $E = B$ and $\mathbf{E} \perp \mathbf{B}$ we have

$$\Upsilon = 2\gamma E/E_{\rm crit} \qquad \text{(constant crossed field)}. \tag{18}$$

At a linear e^+e^- collider a bunch has a radial electric field and azimuthal magnetic field with magnitudes that are essentially equal. Thus the field that induces beamstrahlung is a crossed field, and is approximately constant as viewed by a particular electron in the other bunch. Therefore the proper form of Υ when describing beamstrahlung radiation is eq. (18) and not eq. (17). From ref. [9] I infer that the beam-weighted value of Υ used by Chen and Telnov [3] is based on eq. (18).

If the field is a plane electromagnetic wave the polarization of that wave complicates the expression for radiation by an electron. However, in the limit that the invariant

$$\eta = \frac{eE}{m\omega_0 c} = \frac{e\,|A_\mu|}{mc^2} \tag{19}$$

satisfies $\eta \gg 1$ the radiation is described by the same universal function as for constant fields with Υ as in eq. (16). In eq. (19) ω_0 is the angular frequency of the wave, and A_μ is the 4-vector potential. For a plane wave with 4-vector $\omega_0 = (\omega_0, \mathbf{k}_0)$ we have

$$\Upsilon = 2\gamma E/E_{\rm crit} = \eta\frac{(p\cdot\omega_0)}{m^2} \qquad \text{(plane wave field)}, \tag{20}$$

so the invariants Υ and η are simply related. The limit $\eta \gg 1$ corresponds to the case where many photons from the field interact simultaneously with the electron, with $n \approx \eta^3$ as the typical photon number.[1] For a plane wave with $\eta \gg 1$ the 'radiation length' is much less than a wavelength, so the field is essentially constant during the radiation process and the results for constant fields can be expected to hold. In this limit a plane wave is, of course, to be considered as a constant crossed field.

In E-144 we will not quite be in the large η limit, so there must be some qualifications to the identification between strong laser fields and fields of collider bunches. When we use infrared laser light with $\omega_0 = 1.17$ eV, we have

$$\Upsilon = 0.45\eta, \qquad (\lambda_0 = 1.06\ \mu\text{m},\ p_0 = 50\ \text{GeV}), \tag{21}$$

so if we achieve $\Upsilon = 1$ then $\eta = 2.2$, and the typical number of laser photons absorbed in the radiation process is $\eta^3 = 11$. From Fig. 16 in sec. 90 of ref. [6] (which is for constant fields), or even better, from Fig. 4 of ref. [10] (reproduced as Fig. 8of this note) we infer that when $\Upsilon = 1$ the radiation rate is $\sim 1/6$ of that expected by extrapolation from low field strengths.

For weak fields we can use the Larmor formula to calculate the radiation rate

$$I = -\frac{dU}{dt} = \frac{2}{3}e^2a^{\star 2} = \frac{8}{3}\frac{e^4\gamma^2E^2}{m^2} = \frac{8\pi}{3}\frac{\alpha\eta\Upsilon}{\lambda_0}U, \tag{22}$$

[1]This shows the close relation to synchrotron radiation where $n \approx \gamma^3$ is the typical number of virtual photons scattered to form the radiated photon. For a plane wave with $\eta \gg 1$, the transverse motion imparted to an electron is described by $\gamma \approx \eta$, so the analogy to synchrotron radiation is quite precise in this limit.

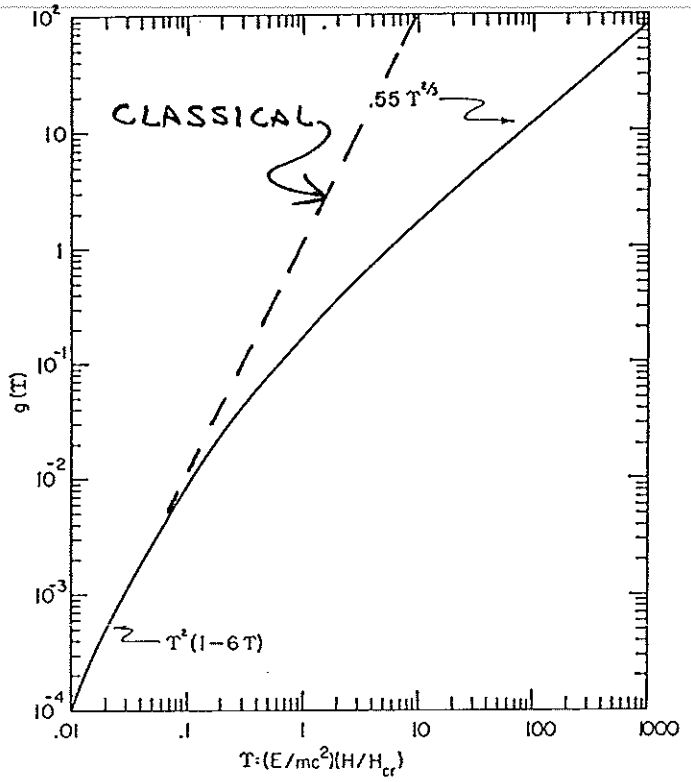

Figure 8: The total rate of emission of photons by an electron in a strong field, presented in the form $g(\Upsilon) = \Upsilon^2 I/I_{\text{classical}}$. Taken from Fig. 4 of ref. [10].

using $a^\star = \gamma^2 a$ and $a = 2eE/\gamma m$ for the transverse acceleration, and noting that $U = \gamma m$ is the initial electron energy. If we define the radiation length by

$$\frac{dU}{dt} \equiv -\frac{U}{\lambda_{\text{rad}}}, \tag{23}$$

then

$$\lambda_{\text{rad}} = \frac{3}{8\pi}\frac{\lambda_0}{\alpha\eta\Upsilon}\left(= \frac{3}{4\pi}\frac{\gamma\lambda_C}{\alpha\Upsilon^2}\right), \qquad (\eta \ll 1). \tag{24}$$

If for $\eta \gg 1$ we use eq. (90.27) of ref. [6] then we have

$$I = 0.37\alpha m^2\Upsilon^{2/3} = 4.6\frac{\alpha\eta}{\Upsilon^{1/3}\lambda_0}U, \tag{25}$$

so that

$$\lambda_{\text{rad}} = 0.22\frac{\Upsilon^{1/3}\lambda_0}{\alpha\eta}\left(= 0.43\frac{\gamma\lambda_C}{\alpha\Upsilon^{2/3}}\right), \qquad (\eta \gg 1). \tag{26}$$

Comparing eq. (25) with Fig. 4 of ref. [10] we see that the strong-field approximation overestimates the radiation rate by a factor of 3 at $\Upsilon = 1$.

After correcting eq. (24) or (26) to apply at $\Upsilon = 1$ the radiation length is

$$\lambda_{\text{rad}} \approx \frac{0.75\lambda_0}{\alpha\eta} \approx 50\ \mu\text{m} \qquad (\Upsilon = 1,\ \lambda_0 = 1.06\ \mu\text{m}). \tag{27}$$

If we focus the laser beam with a mirror with $f/D = 5$ then the Rayleigh range is

$$z_0 = \pi\lambda_0(f/D)^2 = 83\ \mu\text{m}, \tag{28}$$

so the laser presents about 4 radiation lengths to the incident electrons. Therefore multiple interactions must be taken into account, which has not yet been done in any analysis.

5.2 Pair Creation by a High-Energy Photon

In discussing the scattering of laser photons by unpolarized electrons the polarization state of the laser did not enter in the limit $\eta \gg 1$. However, when considering pair creation in collisions between laser photons and a high-energy photon the results depend on the polarizations of both the high-and low-energy photons. Calculations have been made for linearly polarized high-energy photons colliding with a linearly polarized laser [4], unpolarized high-energy photons colliding with a circularly polarized laser [1], for unpolarized photons incident on a static magnetic field [6, 8, 10, 11], and the earliest calculation [12] is for linearly polarized photons incident on a static crossed field.

In the limit $\eta \gg 1$ for a laser field, pair creation in the collision of unpolarized high-energy photons with an unpolarized or circularly polarized laser is described by the same function of Υ (suitably defined below) as for unpolarized high-energy photons in a constant magnetic field [5].

In both E-144 and beamstrahlung at a linear collider the high-energy photons are produced by backscattering low-energy (or virtual) photons off an unpolarized electron beam. In these processes the high-energy photons take on polarization defined by that of the low-energy photons. If the low-energy photons are linearly polarized, then to a very good approximation so the backscattered high-energy photons assume the same linear polarization. [The approximation is best for the highest-energy photons, which are of particular interest in E-144.] When the low-energy photons are circularly polarized, so are the high-energy backscattered photons, but with the opposite handedness.

Hence beamstrahlung photons are linearly polarized, as they are produced from scattering off the virtual photons of the radial electric field of the oncoming bunch. Beamstrahlung pair creation then occurs with high- and low-energy photons of the same linear polarization.

In E-144 the laser beam can be either linearly or circularly polarized. In principle it will be possible to change the polarization of the laser between the first and second collision points if these are spatially separated. In the beamstrahlung part of E-144, however, only a single collision point is used, so the polarization combinations are either both linear, or both circular but opposite.

Calculations for the case of both photons circularly polarized have not been published, to my knowledge, but no doubt could be made by a modest extension of the method of ref. [1].

Certainly the closest correspondence between E-144 and beamstrahlung pair creation will hold for a linearly polarized laser.

The estimate of beamstrahlung pair creation by Chen and Telnov [3] identifies this with pair creation by unpolarized photons in a magnetic field. They used, I believe, the equivalent of eq. (91.10) of ref. [6] for the total pair rate. The more proper version for aligned, linearly polarized photons replaces the factor $2/\kappa$ by $3/\kappa$ multiplying $\Phi'(x)$, comparing to eq. (43) of

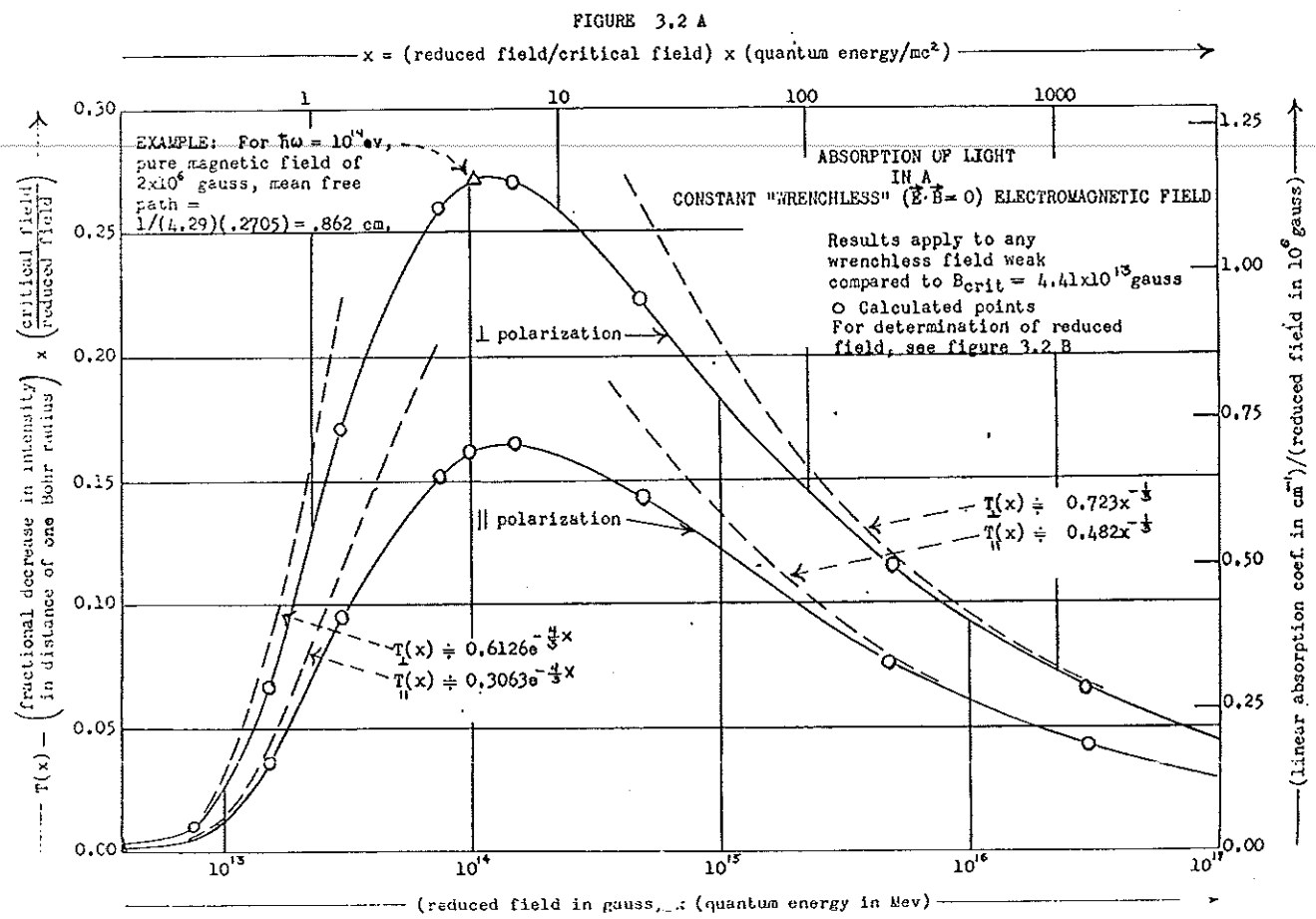

Figure 9: The functions $T(\Upsilon)$ that appear in the expression for the rate of pair creation in strong fields. Taken from fig. 3.2A of ref. [12].

ref. [5] or eq. (3.3-12) of ref. [12]. For $\Upsilon \ll 1$ the rate for aligned, linearly polarized photons in 2/3 that for unpolarized photons, while for $\Upsilon \gg 1$ the factor is 4/5. We infer that near $\Upsilon = 1$ the estimate of Chen and Telnov is perhaps 25% high.

Pair creation by a high-energy photon may be characterized by a radiation length that varies roughly inversely with Υ for Υ between 1 and 100. [Υ for pair creation should be defined as in eq. (16) with p_μ as the 4-vector of the high-energy photon.] For pair creation by linearly polarized photons aligned with a linearly polarized laser we can use eq. (91.12) of ref. [6], or better, eq. (3.3-12) and Fig. 3.2A of ref. [12] (reproduced as Fig. 9 in this note) to write

$$\lambda_{\rm rad} \approx \frac{\lambda_0}{4\pi\alpha\eta T_{||}(\Upsilon)} \left(= \frac{\lambda_C \omega/m}{2\pi\alpha\Upsilon T_{||}(\Upsilon)} \right) \approx 130\ \mu{\rm m} \qquad \text{(pair creation)}, \tag{29}$$

using $\Upsilon = 2(\omega/m)E_{\rm laser}/E_{\rm crit} = 2\omega\omega_0\eta/m^2 = 0.5$ for $\eta = 2.2$ and $\omega = 25$ GeV which is near the endpoint for photons backscattered from a laser with $\lambda_0 = 1.06\ \mu$m by a 50-GeV electron beam. Since $\lambda_{\rm rad}$ is about 2/3 of the full width of the laser pulse there is a small chance of multistep electromagnetic cascade.

Thus a potentially serious shortcoming of the discussion of beamstrahlung in the E-144 proposal (and elsewhere) is that beamstrahlung pair creation was estimated in the thin-radiator approximation. As noted by Erber [10] this permits a closed-form expression for

the two-step process of photon emission followed by pair creation in a strong field. It was assumed that the electron beam is not significantly attenuated, and that a created e^+e^- pair does not suffer any scattering on exiting the bunch. While this may hold for desirable ranges of collider parameters, it is not true in general once $\Upsilon > 1$. Likewise, in E-144 we may well operate in the regime $\Upsilon \gtrsim 1$ where the laser beam appears to be so many radiation lengths thick that an electromagnetic cascade ensues. To date there are no calculations of such cascades, which likely will have to be done via a Monte Carlo method.

6 References

[1] N.B. Narozhnyi, A.I. Nikishov and V.I. Ritus, *Quantum Processes in the Field of a Circularly Polarized Electromagnetic Wave*, Soviet Physics JETP **20** (1965) 622; see also sec. 101 of ref. [6].

[2] F.W. Lipps and H.A. Tolhoek, *Polarization Phenomenon of Electrons and Photons*, Physica **20** (1954) 85, 395.

[3] P. Chen and V.I. Telnov, *Coherent Pair Creation in Linear Colliders*, Phys. Rev. Lett. **63** (1989) 1796.

[4] A.I. Nikishov and V.I. Ritus, *Quantum Processes in the Field of a Plane Electromagnetic Wave and in a Constant Field. I*, Sov. Phys. JETP **19** (1964) 529.

[5] A.I. Nikishov and V.I. Ritus, *Pair Production by a Photon and Photon Emission by an Electron in the Field of an Intense Electromagnetic Field and in a Constant Field*, Sov. Phys. JETP **25** (1967) 1135.

[6] V.R. Berestetskii, E.M. Lifshitz and L.P. Pitaevskii, *Quantum Electrodynamics*, 2nd ed., (Pergamon Press, 1982).

[7] I.M. Ternov, V.G. Bagrov and A.M Khapaev, *Radiation of a Relativistic Charge in a Plane Wave Electromagnetic Field*, Ann. Phys. **22** (1968) 25.

[8] A.A. Sokolov and I.M. Ternov, *Radiation from Relativistic Electrons*, American Institute of Physics (New York, 1986), sec. 24.3.

[9] R.J. Noble, *Beamstrahlung from Colliding Electron-Positron Beams with Negligible Disruption*, Nucl. Instr. Meth. **A256** (1987) 427.

[10] T. Erber, *High-Energy Electromagnetic Conversion Processes in Intense Magnetic Fields*, Rev. Mod. Phys. **38** (1966) 626.

[11] N.P. Klepikov, JETP **26** (1954) 19.

[12] J.S. Toll, *The Dispersion Relation for Light and Its Application to Problems Involving Electron Pairs*, Ph.D. thesis, Princeton U. (1952, unpublished).